

# Key Findings from the NEOSSat Space-Based SSA Microsatellite Mission

**Robert (Lauchie) Scott, PhD, P.Eng.**

*Defence R&D Canada Ottawa, 3701 Carling Avenue, Ottawa, ON, K1A 0Z4*

**Stefan Thorsteinson, M.Sc.**

*Calian Inc. 340 Legget Dr, Ottawa, ON, Canada, K2K 1Y6*

## ABSTRACT

The Near-Earth Orbit Surveillance Satellite (NEOSSat) is a microsatellite space telescope designed to track resident space objects and perform asteroid astronomy. Defence R&D Canada, in partnership with the Canadian Space Agency, developed NEOSSat to perform the HEOSS (High Earth Orbit Space Surveillance) Space Situational Awareness (SSA) mission and the NESS (Near Earth Space Surveillance) asteroid astronomy mission supporting research activities in the Canadian Department of National Defence and supporting Canadian astronomy. A space surveillance satellite orbiting in Low Earth Orbit (LEO) provides advantages for Canadian SSA operations. For instance, the microsatellite's ability to observe resident space objects uninterrupted by the day-night cycle while being unaffected by terrestrial weather offers frequent tracking opportunities compared to ground-based sensors. A space-based sensor also provides the ability for Canada to monitor geosynchronous objects outside of Canadian geographic longitudes adding strategic value for Canadian SSA. In this paper, we discuss some of the key SSA lessons-learned using a microsatellite for SSA metrics, geosynchronous object characterization, and stressing orbital environment factors for optical satellite tracking from LEO. NEOSSat is now beginning an expanded mission phase. A description of some of the more unique experimentation, including observations of space objects conjuncting with NEOSSat itself and high value space asset monitoring is described.

## 1. INTRODUCTION

The success of the MIT Lincoln Lab's Space Based Visible (SBV) program [1] inspired Canada to contribute to US Space Surveillance Network (SSN) using a space-based capability. Recognizing that Canadian ground-based radar would overlap US capabilities and that Canadian weather would reduce the effectiveness of optical telescopes, a space-based option was pursued by the Department of National Defence. The Sapphire project, Canada's operational space surveillance capability, was created under the Department of National Defence [2] envisioning a small satellite system contributing space surveillance data helping Canada achieve its commitments under the Committee for the Peaceful Uses of Outer Space and, eventually, as a contributor to the Combined Space Operations partnership.

The emergence of increasingly available secondary launch rideshare, low-cost small-satellite components and a growing recognition of the space debris problem prompted Defence R&D Canada (DRDC) to examine the viability of even smaller *microsatellites*<sup>1</sup> for Canadian Forces use. DRDC initiated the design studies of *DNESS* (Defense Near Earth Space Surveillance) mission to begin exploring these possibilities. In 2004, funding support was granted when *DNESS* merged with the Canadian Space Agency's (CSA) asteroid astronomy mission Near Earth Space Surveillance (*NESS*). The dual-mission microsatellite, now renamed Near Earth Orbit Surveillance Satellite (*NEOSSat*), began its development and construction in Canada.

DRDC, in partnership with the CSA developed NEOSSat to perform the High Earth Orbit Space Surveillance (HEOSS) Space Situational Awareness (SSA) technology demonstration mission. NEOSSat's HEOSS mission focuses on space-based characterization of deep-space, Resident Space Objects (RSOs) in geosynchronous (GEO) orbit from an observer orbiting in Low Earth Orbit (LEO). A space surveillance satellite orbiting in LEO provides advantages for Canadian SSA operations. For instance, the ability to observe uninterrupted throughout the day-night cycle, the ability to observe regardless of terrestrial weather, and the ability to observe geosynchronous objects outside of Canadian geographic longitudes adds strategic value to these platforms.

---

<sup>1</sup> Microsatellites are small satellites with a mass less than 100 kg and manufactured from commercial-grade electronic parts by small, experienced teams emphasizing a "build-early, test-often" approach.

The story of NEOSSat is a mix of lessons-learned in the development of the microsatellite accentuated with compelling experimental successes in SSA. A small space telescope tracking space objects requires engineering considerations not commonly encountered by the small telescope SSA community. In this paper, an introduction to the operation of a space-based SSA microsatellite is introduced and we discuss the key findings of the microsatellite's performance such as metrics, and measurements of some of the unique orbital environmental issues encountered in space. Some of the new mission areas that NEOSSat is now just beginning to explore are also described such as High Value Asset (HVA) monitoring and observations of objects conjuncting with NEOSSat itself.

## 2. THE NEOSSAT SSA MICROSATELLITE OVERVIEW

NEOSSat was developed by Microsatellite Systems Canada Incorporated (MSCI) and is based on the MOST microsatellite [3] bus. NEOSSat weighs 72 kg with bus dimensions of 0.9 x 0.3 x 0.6 meters with a beveled cylindrical baffle extending another 0.5 meters beyond the +X face of the microsatellite. The spacecraft's payload is a 15 cm on-axis visible light Maksutov telescope fixed to the satellite body. This instrument provides a field of view of 0.8x0.8 degree<sup>2</sup> using a passively cooled E2V 47-20 AIMO CCD detector. A separate E2V 47-20 CCD is mounted adjacent to the main science detector acting as a co-boresighted star tracker enabling fine guidance during tracking of RSOs and celestial objects. The microsatellite is based on a tray-stack design where the avionics and spacecraft subsystems' enclosures are sandwiched such that the avionics trays become the physical backbone of the microsatellite. The microsatellite uses reaction wheels to slew the telescope and relies on the star tracker and embedded quartz rate sensors to perform fine guidance when imaging in inertial (star stare mode) or during fine slews (track rate mode). NEOSSat's payload is fitted with a beveled external baffle to reduce stray light reflected into the instrument enabling observations within 45 degrees from the Sun. This feature was added for the asteroid mission of NEOSSat to enable searching for asteroids near the Sun.

The NEOSSat ground system uses the St Hubert and Saskatoon S-band antennas operated by MacDonald Detwiller and Associates (see Fig.2). The CSA Mission Operation Centre (MOC) provides command checking and telemetry services and commands are up linked via the two ground stations. A Mission Planning System (MPS) manages imagery from NEOSSat and stamps precise orbital ephemeris in the image headers enabling the HEOSS metrics capability. Tasking is performed by scripting time-tagged command macros authored by science users at DRDC or the University of Calgary. NEOSSat is generally tasked 2 days in advance of a script's command execution on orbit to allow for ground station pass opportunities and for command checking prior to upload to the vehicle.

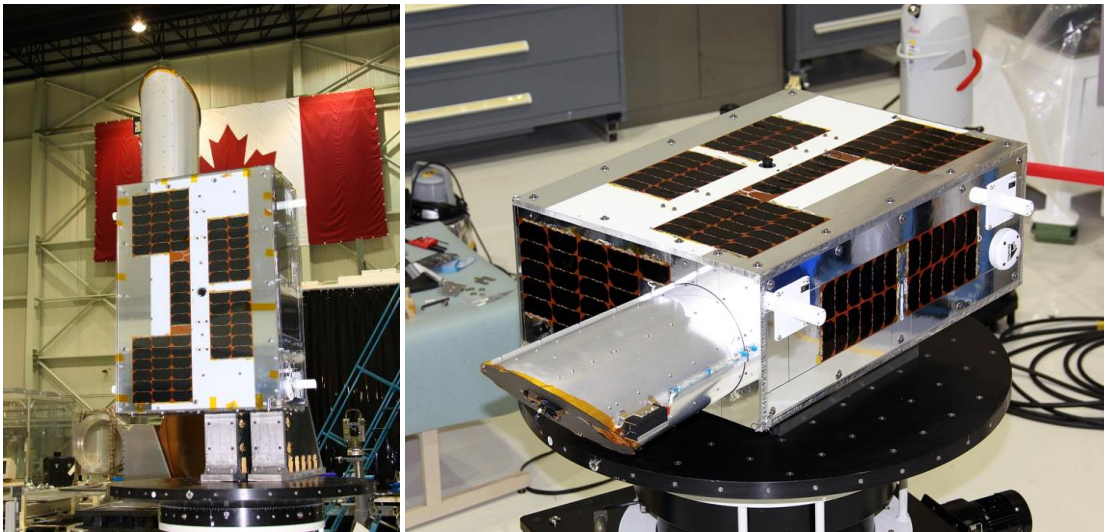


Fig.1 (Left): The NEOSSat microsatellite (Right): NEOSSat emphasizing the beveled telescope baffle

Table 1 – NEOSSat microsatellite overview

<u>Orbit</u>		
Launched:		25 Feb 2013
Orbit:		785 x 785 km. 98° (100 min period) Local Time of Ascending Node: 18h
<u>Satellite general</u>		
Mission class:		Microsatellite space telescope
Mass:		72 kg
Size:		0.90 x 0.33 x 0.65 m (bus) 1.4 m overall length with baffle
Configuration:		Tray-stack avionics
Power (orbit average)		32W (61W peak)
Peak Tracking Rate		60 arcsec/sec
Tracking Telemetry and Control		S-band (2 Aeroastro TTX nodes)
Orbital ephemeris		Novatel OEMV1G GPS receiver 2 meter accuracy
Attitude Control System		Co-boresighted star tracker, coarse Sun sensor with main telescope and reaction wheels. Magnetometer and magnetorquer (inoperable since 2016). GPS enabled attitude enabled in 2017.
<u>Payload</u>		
Optical configuration:		On-axis Makustov Visible imager
Aperture:		15 cm
Field of View		0.8° x 0.8°
<u>Detector</u>		
CCD:		E2V CCD4720 AIMO
Pixel Scale:		3 arcsec/pixel
Peak QE:		0.55 @ 550 nm
Read Noise:		20 e- (with readout electronics)
Dark Current:		<0.1 e-/pixel/sec (at -35°C)

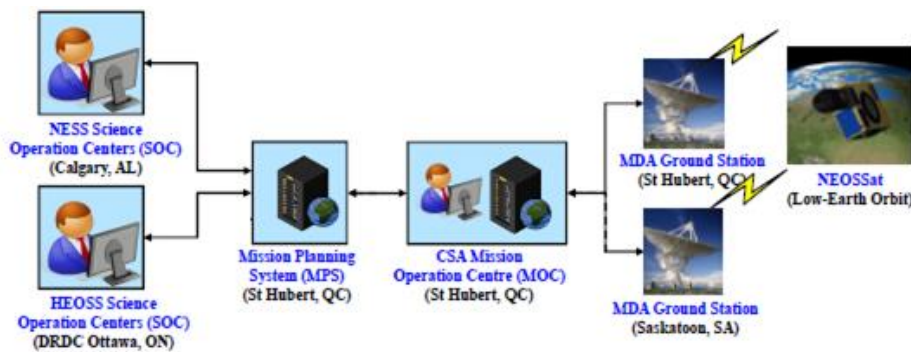


Fig.2 General mission architecture of NEOSSat

There are four primary visibility regions when observing geosynchronous space objects from NEOSSat’s polar orbit. NEOSSat can track objects anywhere outside of the Solar exclusion region, a 90° wide conical region centered on the Sun (red region in Fig.3). NEOSSat’s baffle performance is optimal outside of the Solar exclusion region. Outside of the Solar exclusion region, GEO objects can be tracked up to one-half of an orbital revolution before the

Earth obscures the RSO on either the westward or eastward observing regions. RSOs observed within the Continuous Viewing Zone (CVZ), a region aligned with NEOSSat's orbit normal vector (yellow cone in Fig.3) can observe RSOs for longer periods. This region has the additional property that background stars are always visible to NEOSSat enabling guiding or tracks longer than one orbital revolution. After accounting for NEOSSat's Earth limb grazing angle constraint ( $10^\circ$ ) observations of GEO objects centered within the CVZ can be sustained up to 2.2 hours.

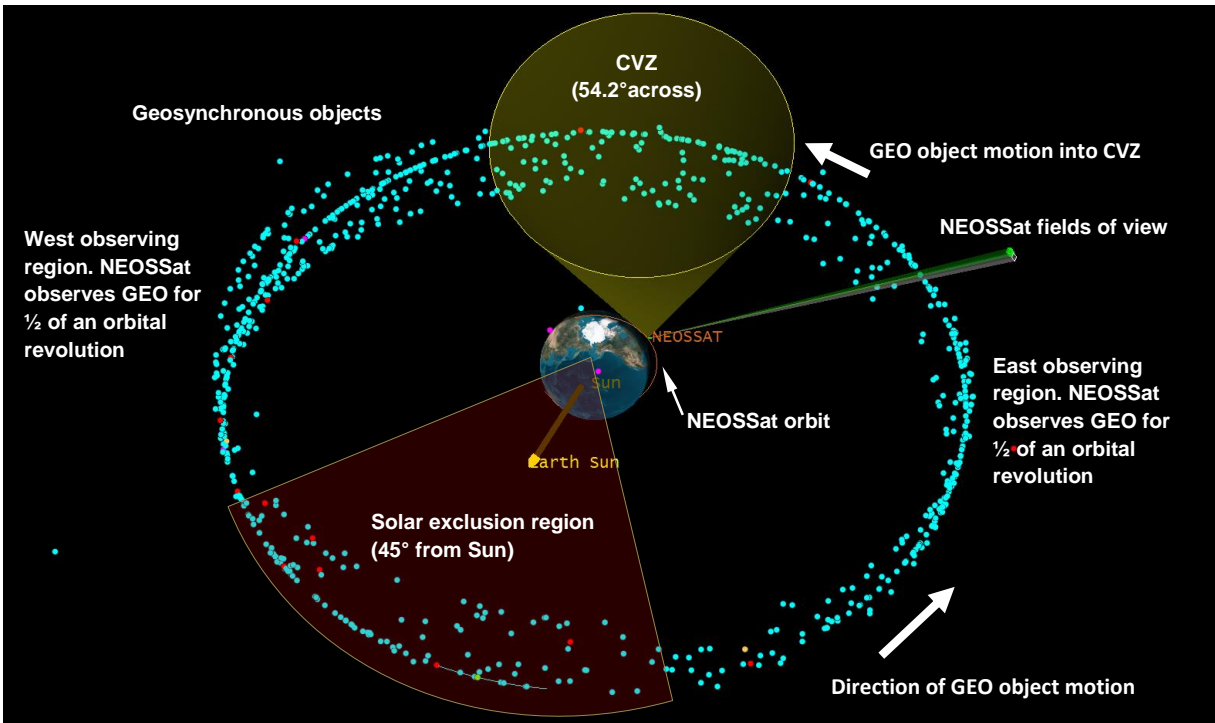


Fig.3 NEOSSat Geosynchronous object observing geometry with Continuous Viewing Zone (CVZ) shown

DRDC Ottawa tasks NEOSSat to track deep space objects of SSA research interest. Most objects are operational geostationary satellites which perform orbital maneuvers, satellites experiencing on-orbit issues, such as the AMC-9 anomaly in 2017, or are orbital derelicts in the disposal orbit approximately 300 km above GEO orbit. During SSA observation planning NEOSSat must respect several constraints due to attitude control system limitations and visibility constraints while observing RSOs with a visible-light sensor. NEOSSat tracks RSOs by Euler-slewing the microsatellite body along the projected direction of an RSO's relative angular motion and acquiring a series of images to complete a track. The constraints and conditions applied during NEOSSat tracking are:

- **NEOSSat Constraints**
  - NEOSSat +X direction of the Science detector is aligned toward the target RSO
  - NEOSSat -Z solar panel is constrained Sunward to maintain power and thermal constraints
  - Instrument radiator points (preferentially) toward deep space
  - NEOSSat is outside of the South Atlantic Anomaly during fine acquisition slew phase
  - Imaging preferably occurs outside of TT&C downlinks with the ground stations
  - NEOSSat's slew destination is not obscured by the Earth during fine-slews
    - Stars must be continuously present during tracking operations
- **Target RSO Constraints**
  - RSO is in direct Sunlight (RSO is outside of eclipse)
  - RSO is brighter than Magnitude 16
- **Line-of-Sight Constraints (Target RSO relative to NEOSSat)**

- RSO-centric phase angle is less than 135 degrees
  - observing inside of the Solar exclusion region is prohibited
- Angular rate of the RSO relative to NEOSSat is  $< 60$  arcseconds/second
- Grazing angle of RSO above the Earth limb is greater than  $> 10$  degrees
- The background of the NEOSSat field of view contains background stars for star tracker operation
  - Background stars are required for astrometric measurement of RSO position
- Lunar and planetary exclusion angles are  $>4$  degrees
- The galactic centre is generally avoided (but not stringently)

Space-based metric observations are reckoned relative to NEOSSat and a Novatel OEMV1G GPS receiver continuously measures NEOSSat orbital position. Simultaneously, this GPS receiver steers the onboard payload clock ensuring sub-millisecond accuracy with respect to UTC. This GPS data is post-processed on the ground achieving 2 meter (3-sigma) orbital accuracy which is more than sufficient for metric measurements on GEO objects.

NEOSSat acquires imagery at a rate of 1 full frame image every 65 seconds in 1x1 binning and one image every 20 seconds in 2x2 binning for short-exposure SSA imaging. This relatively slow rate of image acquisition is due to NEOSSat's asteroid astronomy heritage requiring slow CCD readout enabling faint object detection near the image noise floor. To increase the imaging cadence for SSA, HEOSS observes a fraction of the NEOSSat frame enabling an imaging rate of 1 RSO image every 45 seconds at the resolution of 3 arcseconds per pixel.

### 3. IMAGE PROCESSING, ACCURACY AND SENSITIVITY

Imagery acquired from NEOSSat on geosynchronous RSOs requires specialized image processing to produce accurate metric and photometric observations. Fig. 4 shows a composite of NEOSSat imagery acquired during a single track on geostationary satellites Anik F2 and Wildblue-1 residing at  $111^\circ\text{W}$ . The satellites are identifiable as larger point sources on the imagery, however there are numerous sporadic point sources on subsequent images. These sporadic point sources are high energy particle strikes impacting the detector during imaging operations. These particle strikes render classical pixel-clustering detection techniques ineffective and the NEOSSat image processing must accommodate their presence. HEOSS' space surveillance imaging processing system Semi-Quick Intelligent Detection (SQUID3) uses a combined matched filter and stacking algorithm to simultaneously reject particle strikes, detect and centroid the background star streaks and produce space surveillance observations consisting of J2000 right ascension, declination and time. The detected magnitude of the RSO is also recorded and stored in the SQUID3 image processing database.

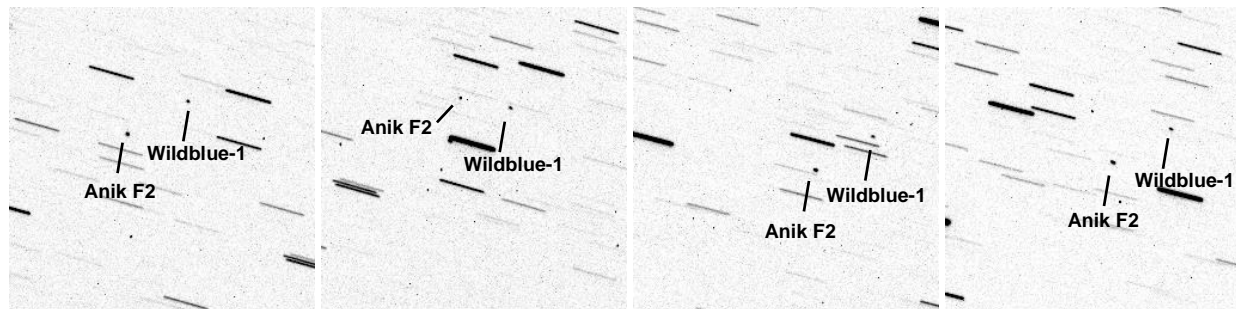


Fig.4 NEOSSat observations acquired on a single geostationary satellite track (negative image shown). The geostationary satellites are marked for clarity.

**Astrometric Accuracy:** NEOSSat's metric accuracy is assessed by observing GPS satellites using NEOSSat's instrument and comparing these observations to the precise GPS orbital ephemerides available from the Crustal Dynamics Data Information team as ".sp3" ephemerides [4]. Fig. 5 shows the as-built root mean square residuals taken on GPS calibration satellites as measured by NEOSSat in 2016 [5]. The accuracy of both instrument imaging binning modes (1x1 and 2x2) are shown. 2x2 binning increases NEOSSat's imaging rate due to the faster image transfers from the instrument to satellite memory. While 2x2 binned images is expected to have a lowered metric

accuracy and sensitivity the increased imaging rate was viewed as a positive trade-off to help compensate for the lower imaging rate. In 1x1 binning, the instrument shows an overall metric error of  $\sigma = 2.3$  arcseconds and  $\sigma = 3.7$  arcseconds for the 2x2 binning.

Some of the skew noticeable in Fig. 5 (left) is attributed to NEOSSat’s relatively long tracking intervals where the first and last observations tend to be elongated. This is due the smearing of the targeted point-source of the RSO during tracking where the targets’s relative acceleration mismatches the constant angular rate Euler slew NEOSSat uses during tracking. This effect smears the RSOs at the start and end of a track (see Fig. 6). If NEOSSat could image at a rate faster than one image every 45 seconds the relative angular velocity difference could be constrained to less than one pixel. This would alleviate the smearing in NEOSSat imagery and in the skew in NEOSSat metric data.

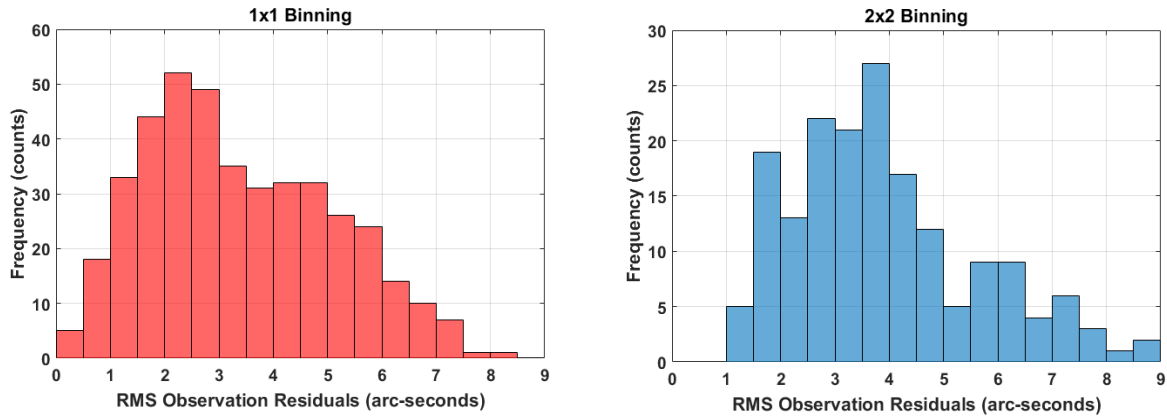


Fig.5 NEOSSat (HEOSS) mission RMS metric accuracy histograms [5]

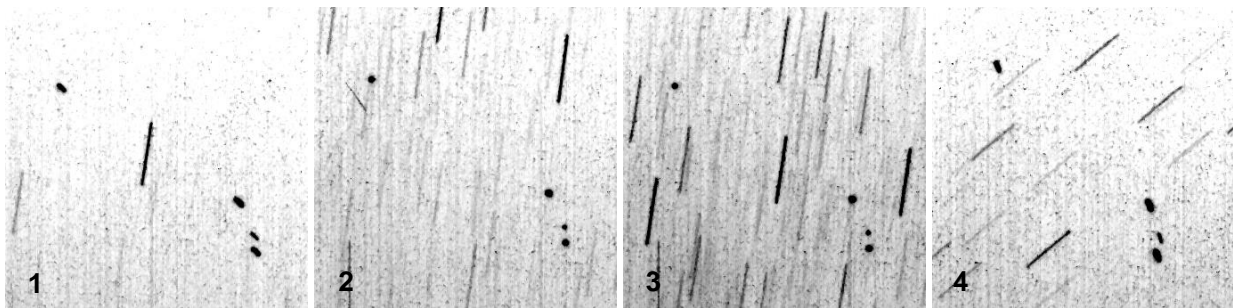


Fig.6 NEOSSat track on Echostar 17, Anik F1, Anik F1R and Anik G1. The satellites show point source smearing at the start (1) and finish (4) of the track.

A lesson learned in the calibration of NEOSSat’s metric accuracy is that the low tracking rate of NEOSSat’s attitude control system (60 arcsec/sec) limits the number of detectable GPS calibration satellites on any given day. This causes the assessment process to take a month or more to collect enough measurements to make meaningful statistics. The GPS constellation’s mean orbital speed relative to NEOSSat’s incurs an average angular rate of 78 arcseconds/second and a minimum possible angular rate of 30 arcsec/sec. This limits the number of observing opportunities making NEOSSat metric calibration difficult and relatively time consuming. Future space surveillance missions are recommended to ensure their attitude control systems can track at rates greater than ~120 arcsec/sec to ease the metric accuracy assessment process by expanding the number of accessible GPS satellites at any given time.

**Photometric Sensitivity:** NEOSSat can detect magnitude 16 RSOs using frame stacking [5] and is the standard image processing technique applied to NEOSSat imagery. Fig. 7 shows the detected magnitude of all NEOSSat GEO detections from 2016 to 2018. The spike near magnitude 11.5 (Fig. 7 left) reflects the brightness peak of the GEO satellite population commonly reported by many GEO satellite observers. NEOSSat can detect RSOs fainter than magnitude 16 by adjusting exposure times and stacking approaches, but the system is largely insensitive to the secondary population of debris objects known to exist in GEO orbit [6] fainter than magnitude 17. Future space surveillance missions maintaining the deep space catalog should consider the ability to detect smaller debris-sized objects to help maintain custody of smaller satellites expected to appear in the GEO regime in the coming years and other debris objects known to be in the deep space geosynchronous regime. Fig 7 (right) shows the phase angle distribution for these observations. The spike reflects a minor tendency of the HEOSS tasking system to plan observations at lower phase angles on the western observing region of GEO.

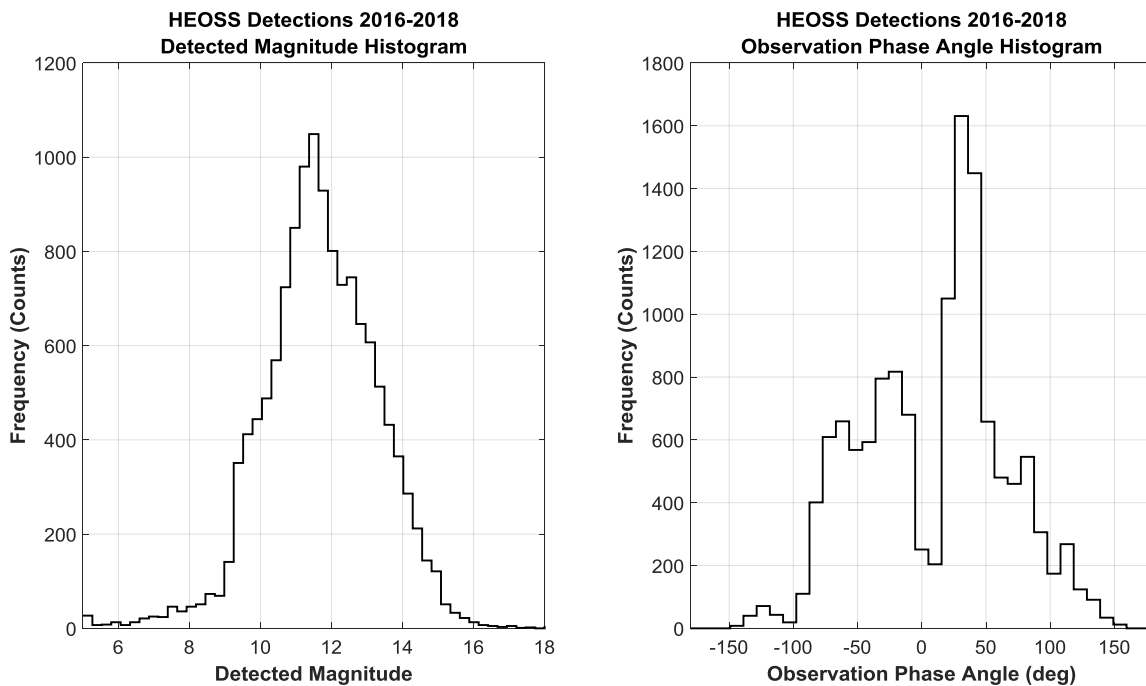


Fig.7 (Left): NEOSSat (HEOSS) mission photometric distribution of all detected GEO objects (Right): Distribution of the phase angles of the observations

Fig. 8 shows all NEOSSat photometric observations on GEO objects versus phase angle. The majority of observations occur within the  $\pm 90^\circ$  phase angle regime with a noticeable dip near zero phase due to NEOSSat's line of sight geometry rarely enabling these observations. On the other extreme, NEOSSat routinely reports observations greater than 90 degrees phase angle and has tracked objects within 30 degrees from the Sun inside of the Solar Exclusion region during NEOSSat's eclipse season [7]. Most stabilized GEO satellites tend to fade considerably at these high phase angles and are often fainter than magnitude 16 and is reflected in the plot. NEOSSat can track larger GEO objects on Earth's dayside but is limited by its overall sensitivity.

NEOSSat performs the general space surveillance catalog maintenance role relatively well. NEOSSat's ability to respond to geostationary satellite maneuver events is largely governed by the field of view of the NEOSSat detector and can handle geosynchronous satellite maneuvers up to 0.4 m/s during East/West maneuver operations under the 2-day tasking cadence used by NEOSSat. NEOSSat's ability to respond to sudden, unexpected SSA events could be improved. Large geostationary satellite maneuvers, tagging of fragmentary debris from satellite breakups or helping de-risk a conjunction of a satellite in GEO are events which strains NEOSSat's 2-day tasking cadence. Break up event characterization has not been achieved with NEOSSat with exception of chance observations on the AMC-17

satellite breakup in 2017 after its initially reported mission anomaly. Improved ground station access and an increased rate of command checking would improve tasking responsiveness to such SSA events. Future missions are recommended to increase connectivity to the space segment to help address timeliness for these SSA mission areas.

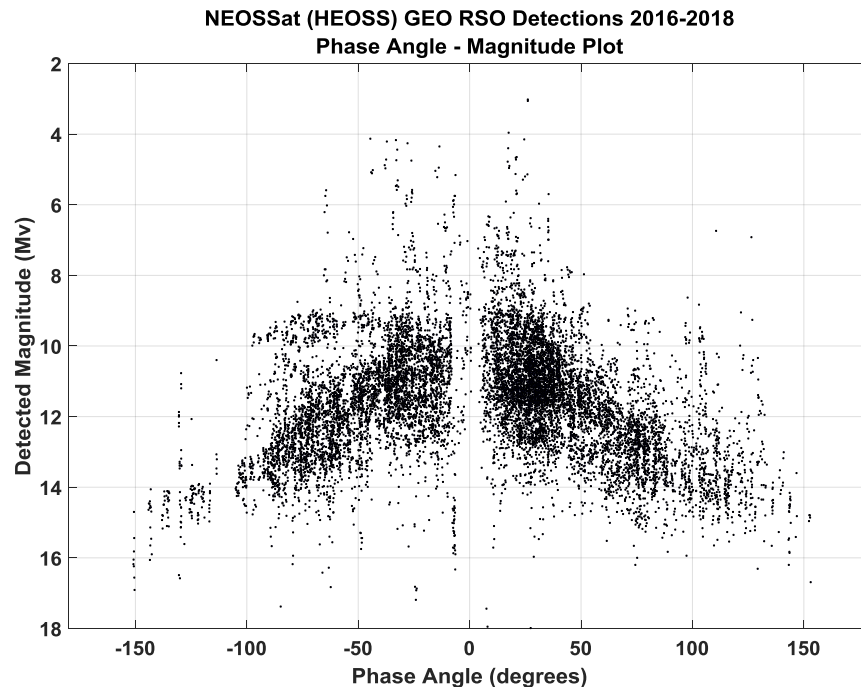


Fig.8 NEOSSat (HEOSS) mission GEO object detected magnitude vs phase angle

#### 4. STRESSING OBSERVING CONDITIONS IN LEO ORBIT

Space-based telescopes can observe deep space RSOs with a high frequency from LEO however they are exposed to unique environmental effects strongly impacting image processing. The two strongest effects are: 1) the South Atlantic Anomaly (SAA) where energetic particles impact the NEOSSat imager within the geomagnetic anomaly over South America and 2) The bright Earth limb illuminated by the Sun, especially during NEOSSat's motion over the Antarctic ice sheet during the Antarctic summer.

NEOSSat's orbital motion inside the SAA routinely subjects the vehicle to high fluxes of charged energetic particles such as high energy protons trapped in this region. These SAA traversals are generally benign and NEOSSat functions normally. From a payload operations perspective, these high energy particle strikes pierce the payload creating sporadic point sources or streaklets on the science detector if images are being acquired. These particle strike blemishes limit the ground system's image processing effectiveness due to the additional "confusion" sources on the imagery. RSOs and particle strikes are difficult to differentiate and Fig. 9 shows the progression of particle strikes during NEOSSat's motion toward the SAA. Fig 9 panel 1 shows normal NEOSSat imaging outside of the SAA followed by entry into an in the center (Fig 9 panel 3) of the SAA. NEOSSat imaging is generally scheduled outside of the SAA to avoid collecting imagery of little processing value and to mitigate this effect. Imaging can occur for special space events, such as an antenna deployment, maneuvers, or if other time-critical tasking is required during NEOSSat's flight in the SAA. Exposures are generally shortened in duration (1 second or so) to help mitigate the number of proton hits on the imager.

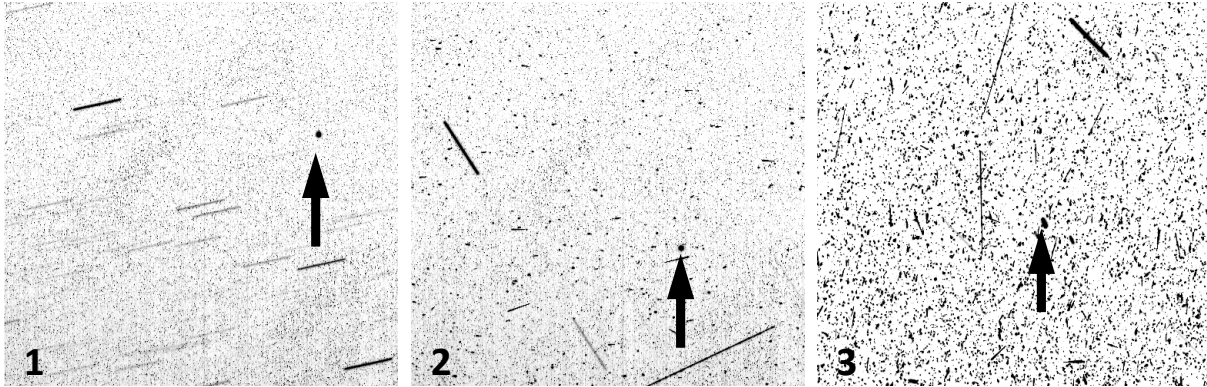


Fig.9: Series of images during NEOSSat’s flight (1) outside of, (2) entering into, (3) at the center of South Atlantic Anomaly. The tracked RSO is marked on the frames. Short line parallel line segments are background stars

It was quickly noticed after NEOSSat’s launch that during winter each year there are very high levels of background brightness encountered during imaging over the South Pole. This is due to sunlight reflecting from the Antarctic ice sheet and subsequently detected by the space telescope. This effect is strongly coupled to NEOSSat’s look angle relative to the Earth limb. To characterize this bright Earth-limb induced background variation, a test was performed aiming NEOSSat’s telescope at selected star fields within the CVZ. The star observations were timed such that the stars’ closest Earth Limb Elevation (ELA) was during NEOSSat’s polar crossings (see Fig. 10). Images were taken over an entire orbit providing a variety of ELA angles to measure the background brightness. The background surface brightness  $M_{bg}$  is measured by subtracting the bias and dark levels from NEOSSat imagery and scaled using to a 1 arcsecond<sup>2</sup> equivalent angular area using

$$M_{bg} = M_0 - 2.5 \log_{10} \left( \frac{Flux/T_{exp}}{\alpha^2} \right) \quad (1)$$

where  $M_0$  is the NEOSSat instrumental zero point (21.6 magnitudes/count),  $Flux$  is the statistical mode of the dark-corrected NEOSSat Science detector imaging area,  $T_{exp}$  is the exposure time of the image and  $\alpha$  is the NEOSSat detector pitch. To capture the seasonal variations of the North and South polar caps two tests were performed One in February 2018 and the other in June 2018. While the winter test was not optimally performed during the winter solstice the measurements provide representative sky brightness for a space-based telescope when observing near this polar extreme.

During normal NEOSSat operations the microsatellite avoids imaging near the illuminated Earth limb by setting a 10-degree grazing angle elevation limit. Fig. 10 clearly shows why this limit is required as the background surface brightness exponentially increases limiting RSO sensitivity and reducing the number of detectable background guide stars for the star tracker. Overlaid on Fig.10 is the Hubble Space Imaging Spectrograph (STIS) reference background brightness guideline [8] and is shown for comparison. There are strong departures from the STIS guideline near the North and South Polar Regions many of which are 3 magnitudes/arcsec<sup>2</sup> in magnitude. During the closest look angle near the Antarctic limb NEOSSat’s detector saturated causing the flattened appearance of measurements between 10 and 13 degrees. Imaging operations can be performed during polar crossings on space objects if the imager stays well above the bright Earth limb (~30°) or if the observations are performed over the seasonally darkened limb.

At ELA angles greater than 25 degrees, neither the Northern nor Southern polar tests show measurements fainter than 21.5 magnitudes/arcsec<sup>2</sup>. Some measurements taken during the Northern pole test suggest backgrounds nearing the Zodiacal “faint” background however there are few measurements achieving this level. This is attributed to the beveled design of the baffle where off-axis Sun-sources are designed to be rejected by the baffle, but Earth limb light sources can enter the unbeveled side reflecting down the instrument toward the detector. There are few observing geometries which mitigate both the bright Sun and Earth sources simultaneously and is a possible cause for the brighter sky brightness measurements reported in Fig. 10.

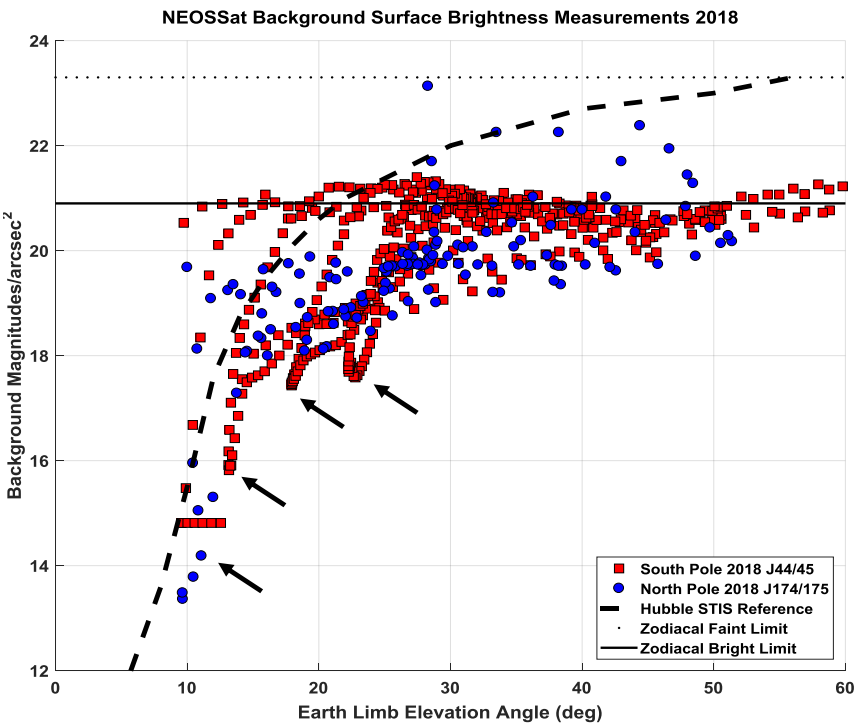
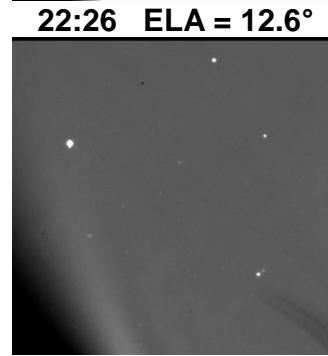
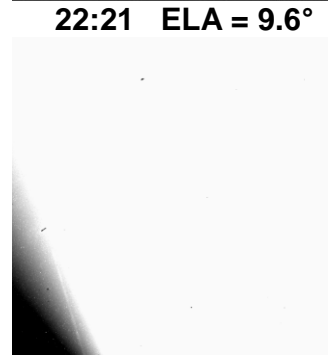
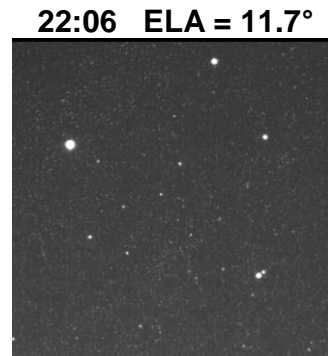
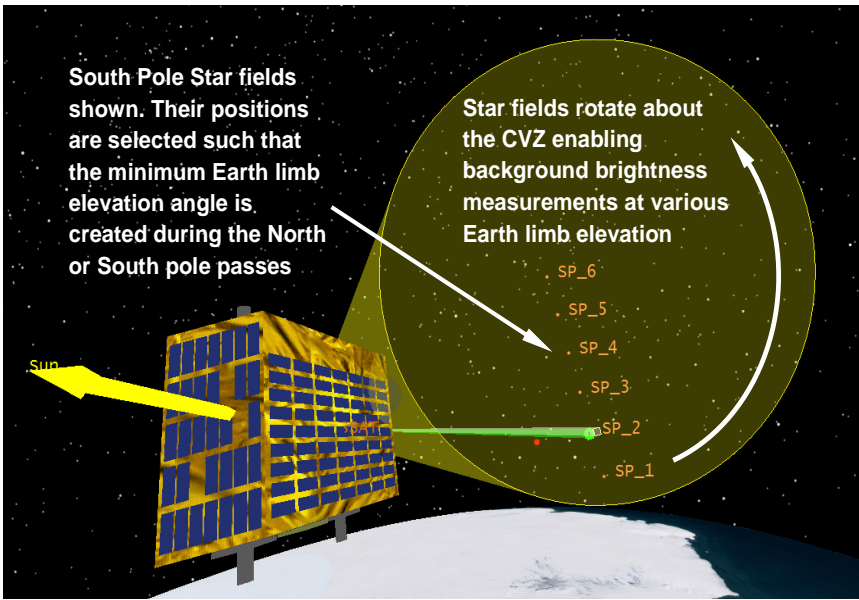


Fig.10 (Top left): NEOSSat test star fields in the CVZ. (Right Column): Images from NEOSSat during a South pole pass showing strong background surface brightness increase during polar crossings at 10° ELA. (Bottom Left): Surface brightness measurements by NEOSSat during Southern (Red) and Northern (Blue) polar crossings. The Hubble Space Telescope Imaging Spectrograph background brightness guideline [8] is shown for comparison.

## 5. NOVEL APPLICATIONS AND NEW AREAS OF SSA EXPLORATION

Most NEOSSat observations satisfy the original deep-space SSA science activities devised for the mission in 2009. NEOSSat is now in an extended mission phase where new SSA applications are being explored taking advantage of NEOSSat's unique in-situ orbital perspective. Some experiments have opened a new orbital class for NEOSSat to observe. For instance, orbital collision risks to NEOSSat itself (e.g. conjuncting space objects) are now being characterized from NEOSSat. Another area showing promise is High Value Asset (HVA) persistent surveillance, where a deputy satellite performing passive long range, co-orbital monitoring of a strategic asset can provide event verification in orbit. Some experimentation in these areas is now described.

**Conjunction Observations:** NEOSSat has begun observing low probability of collision conjunctions between NEOSSat and other space objects. These are unique, short duration and unusual characterization experiments as the primary satellite in a conjunction rarely senses the presence of the fast-moving secondary RSO during its rapid approach or retreat during a conjunction. These observations are possible due to a geometric property of objects on collision trajectories. Such trajectories exhibit motion described as “constant bearing – decreasing range” meaning that the advancing object has very small angular rates during its advance, making it trivial for NEOSSat to acquire before the Time of Closest Approach (TCA). NEOSSat simply points toward a star field in the direction of the rapidly advancing secondary and frames the imager continuously to observe its advance. Conversely, NEOSSat can also observe the star field during a secondary object's retreat from TCA. Photometrically, these short (~250 second) tracks are phase-angle invariant as the Sun and observer lines of sight are relatively constant during the close approach and we show example light curves from these unique measurements.

Fig. 11 shows stacked images of the approach of Orbcomm FM-20 and the retreat of Iridium 17 which made a close approach to NEOSSat on 29 Jun 2018 as forecasted by Socrates service on Celestrak [9]. Orbcomm FM-20 appears as the string-of-pearls object in the stacked images in the upper left of Fig.11. During the last detection, Orbcomm FM-20 flies past NEOSSat and is the bright streak on the image. When a secondary makes its closest approach to a satellite there is a rapid increase in angular rates causing it to streak in these NEOSSat images. The observed light curve of FM-20 during the conjunction is shown in Fig. 11 (right) showing a monotonic increase in brightness during its rapid advance. Interestingly, an inverse square ( $R^{-2}$ ) fit to account for brightness changes due to range does not show good adherence to the measured data. This suggests that Orbcomm FM20's pose deviates its photometric behavior away from the expected range-induced brightening that should be observed. The measurements were collected over the darkened South Pole, so Earth illumination of Orbcomm FM-20 is not believed to be the cause of this deviation in brightness.

Fig. 11 also shows conjunction measurements on Iridium 17 except imagery was acquired just after TCA. This light curve is a bit more unique as evidence of rotational motion of the secondary (oscillating photometry) is visible in Fig 11 (bottom right). Iridium 17 and Orbcomm FM-20 both show detected apparent magnitudes between 10 and 4 during these close approaches with closing ranges of 4000 km or less. Both objects are listed as medium-sized radar cross sections in the space-track catalog [10] suggesting they are  $1\text{m}^2$  or more in size. NEOSSat has attempted detecting debris-sized (~10cm) conjuncting secondaries however these fainter debris objects remain elusive. Assuming an albedo of 10% and a slant range of 3000 km, a 10 cm spherical object would be magnitude 15.4, just below NEOSSat's threshold detection limit. Objects in this debris-size regime remain challenging and work is ongoing to characterize them.

**Medium Range HVA Monitoring:** NEOSSat's orbit is similar to Sapphire's due to their shared launch in 2013. Neither satellite can maneuver so their orbits evolve naturally based on their initial orbital injection from the launch vehicle. Every year, NEOSSat drifts near Sapphire due to the slight difference in orbital period between the two spacecraft. This creates observing windows on Sapphire from NEOSSat enabling the NEOSSat mission team to perform in-situ monitoring of a HVA at medium range (1000-5000 km). NEOSSat observed Sapphire conjuncting with Iridium 16 on 29 Jun 2018 at 09:18 UTC and Fig. 12 (left) shows Sapphire (faint vertical streak) and the rapidly approaching Iridium 16 (brighter streak) during their conjunction. Fig 12 (right) shows the geometry of NEOSSat, Sapphire and Iridium 16 just prior to TCA where NEOSSat was 1940 km from Sapphire. This close approach was observed in sidereal stare and the exposure was timed to coincide with Sapphire and Iridium 16's

TCA. Unfortunately, as the NEOSSat imager frames slowly there is little tracking data<sup>2</sup> that can be obtained on these two spacecraft and work is ongoing to determine if astrometric value is achievable from such imagery.

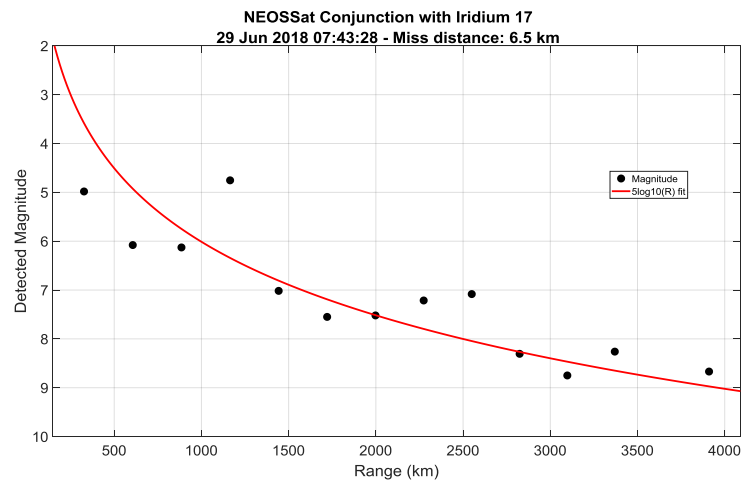
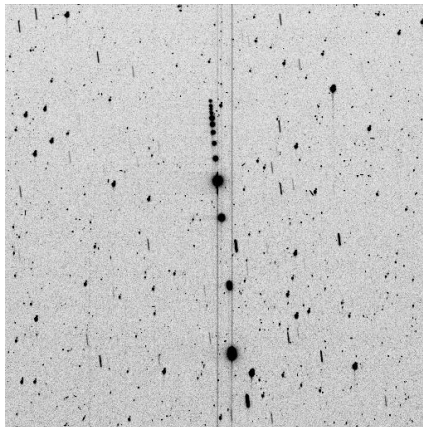
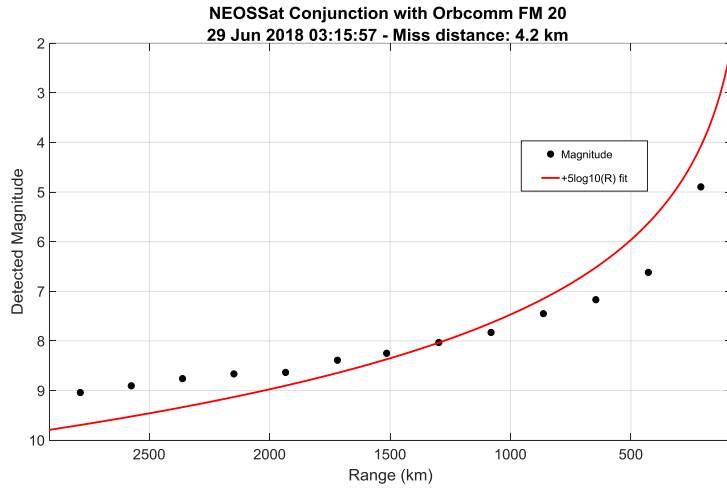
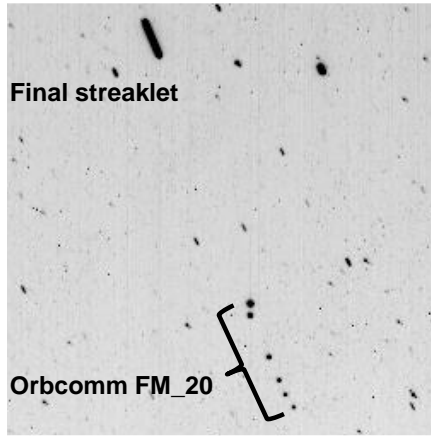


Fig.11 (*Top left*): Stack of NEOSSat frames of Orbcomm FM-20 during its conjunction with NEOSSat. (*Top right*): Photometry of Orbcomm FM 20 showing a departure from an inverse square brightness fit. (*Bottom left*): Iridium 17 stack showing the fade-out of the object just after TCA. (*Bottom right*): Photometry of Iridium 17 suggesting possible rotational motion of the secondary.

<sup>2</sup> This tracking geometry suffers from low in-track observability on Sapphire as NEOSSat is looking down Sapphire's velocity vector.

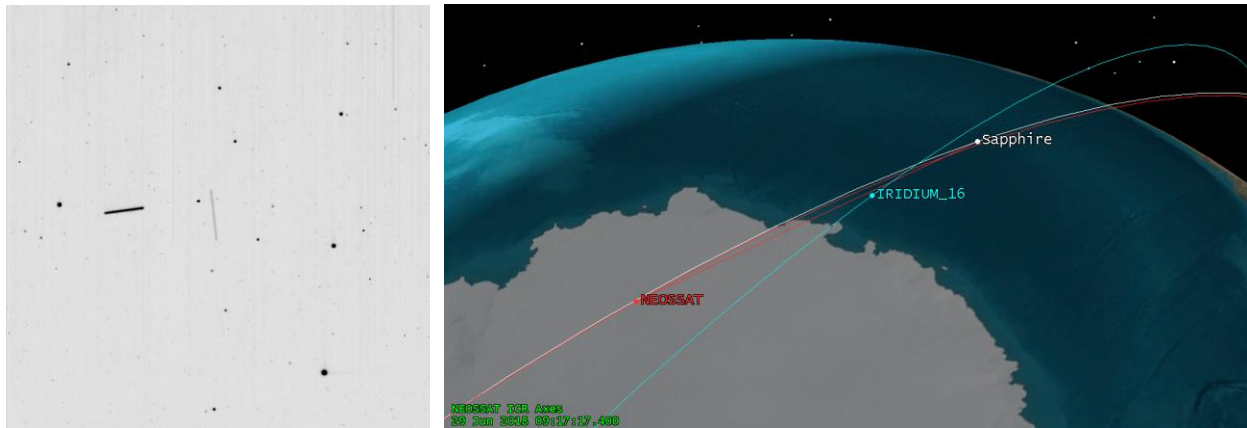


Fig.12 (left): Sapphire (vertical streak) and Iridium 16 conjunction just prior to TCA observed by NEOSSat at a range of 1940 km. (right): Observing Geometry of Sapphire, Iridium 16 and NEOSSat.

Potential applications of this approach could be to validate SSA events occurring on the HVA, such as fragmentations or deployment antennas or other appendances by monitoring the HVA's photometric signature. Despite the orbital observability limitation when observing a satellite in nearly the same orbit as the observer, validation of events occurring on the HVA is a possible application of this medium range tracking approach. Future missions are recommended to use faster imaging framing rates and use a higher ACS tracking rate consistent with the orbital speed of the observer's in orbit. For NEOSSat, this tracking rate would be approximately 216 arcseconds/second and could enable persistent monitoring of the HVA.

**Proximity Observations:** The most dramatic and dynamic observations acquired on Sapphire by NEOSSat occurred during a very close proximity pass when Sapphire's relative angular rate fell within the NEOSSat's ACS tracking limit. In June 2018, NEOSSat tracked Sapphire within 50 km and the resulting images are shown in Fig. 13. NEOSSat is designed for observations on deep space objects therefore the very close proximity of Sapphire created strong bloom spikes due to Sapphire's significant apparent brightness. In some frames, Sapphire cast reflections and shadows of NEOSSat's secondary mirror when the two satellites less than 20 km apart. Relative orbit tracking applications are now being explored as the background stars in such NEOSSat imagery can be used to unambiguously determine the relative position of another satellite near NEOSSat. A new area of exploration, in-situ proximity observations, are now being explored.

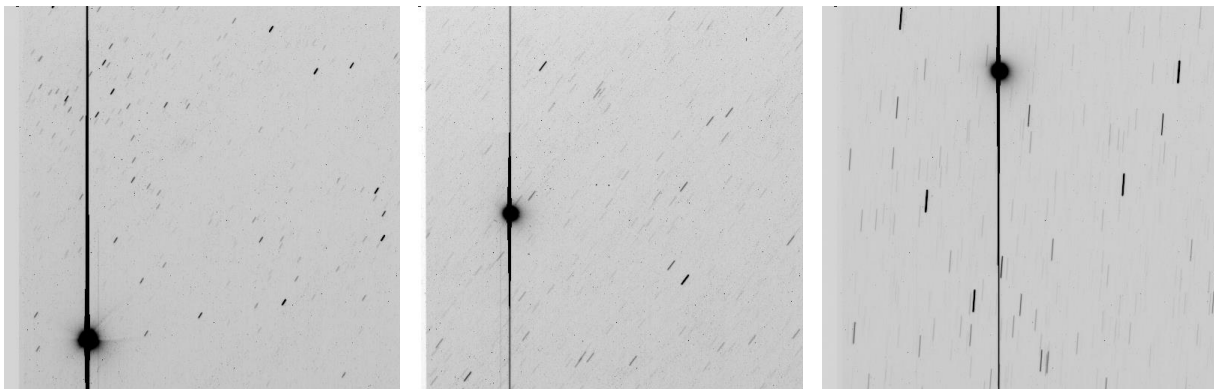


Fig.13 Observations of Sapphire by NEOSSat at slant ranges of 20, 35 and 50 km. Background star trails are visible

## 6. SUMMARY AND CONCLUSION

The NEOSSat microsatellite is continuing to explore the use of microsatellites for Space Surveillance. Several lessons learned in the monitoring and tracking of spacecraft in deep space were achieved. The microsatellite platform is relatively well matched for routine GEO space surveillance tracking sensitive to magnitude 16 objects accurate to 2.3 arcseconds and is comparable to ground-based SSA sensors. The relatively slow framing rate of the NEOSSat imager limits the productivity of the sensor and affects metric accuracy by tending to smear the first and last observations in a sequence. NEOSSat's 2-day tasking lead time and image download cycle makes NEOSSat less responsive to sudden SSA events such as maneuvers, breakups or performing collision assessment observations. It is recommended that future microsatellite space surveillance missions strive for real-time tasking to improve responsiveness. The stressful observing conditions that NEOSSat encounters when operating within the South Atlantic Anomaly reduces the amount of time that observations can take place and mitigation measures are described to help maintain tracking operations in this region. NEOSSat has characterized the polar brightness environment showing the exponential increase in background surface brightness when observing RSOs near Earth's illuminated limb. Observations taken over the illuminated North and South poles show background surface brightness exceeding 14 magnitudes/arcsec<sup>2</sup> when observing within 10 degrees of Earth's illuminated limb.

New, in-situ orbital applications of NEOSSat are now being explored. The microsatellite has conducted what we believe are the first, primary-satellite based observations of a fast-approaching secondary object during a conjunction and light curves for these objects are shown. New medium-range observations of HVAs are now being explored and a conjunction event on Sapphire by Iridium 17 was observed by NEOSSat. Proximity observations of Sapphire with slant ranges less than 50 km have been achieved and these observations are now being probed for their astrometric value. The NEOSSat mission team looks forward to continued and expanded experimentation by attempting new imaginative applications for the SSA community. There's no better place for doing SSA than in space.

## 7. ACKNOWLEDGEMENTS

The authors wish to acknowledge the tremendous support for the NEOSSat mission by the Canadian Space Agency, Satellite Operations Team and the marvelous efforts by Microsatellite Systems Canada and Magellan Aerospace for their incredible work reviving the NEOSSat microsatellite from a significant subsystem failure in 2016. The authors also wish to acknowledge the support from The Royal Canadian Air Force - Director General Space, the Sapphire Satellite Operations Centre at 22 Wing North Bay, the Canadian Space Operations Centre (CanSpOC) in Ottawa and Assistant Deputy Minister of Science and Technology for their support of the NEOSSat mission.

## 8. REFERENCES

- 1 Stokes, G.H., von Braun, C., Ramaswamy, S., Harrison, D., Sharma, J., "The Space Based Visible Program", Lincoln Lab Journal, Vol.11, No. 2, (1998).
- 2 Maskell, P., Oram, L., "Sapphire: Canada's Answer to Space-Based Surveillance of Orbital Objects", AMOS Technical Conference, Maui, HI, 2008.
- 3 Walker, G., Matthews, J., Kuschnig, R., Johnson, R., Rucinski, S., Pazder, J., Burley, G., Walker, A., Skaret, K., Zee, R., "The MOST Astroseismology Mission: Ultraprecise Photometry From Space", Publications of the Astronomical Society of the Pacific, Vol. 114, pp 1023-1035, Sept 2003.
- 4 Crustal Dynamics Data Information team, sp3 orbital ephemerides, [https://cddis.nasa.gov/Data\\_and\\_Derived\\_Products/GNSS/orbit\\_products.html](https://cddis.nasa.gov/Data_and_Derived_Products/GNSS/orbit_products.html) accessed March 2017.
- 5 Thorsteinson, S., "Space Surveillance from A Microsatellite – Metric Observation Processing from NEOSSat", Masters Thesis, Royal Military College of Canada, accessible from <http://hdl.handle.net/11264/1364>, June 2017.
- 6 Schildknect, T., Musci, R., Flury, W., Kuusela, J., de Leon, J., de Fatima Dominquez Palmero, L., "Optical Observations of Space Debris in High Altitude Orbits", Proceedings of the 4<sup>th</sup> European Conference on Space Debris, ESA SP-587, Darmstadt, Germany, 18-20 April 2005.
- 7 Thorsteinson, S., Scott, R.L., "NEOSSat Space Situational Awareness Case Study: GOES 16 Relocation Tracking" CASI ASTRO 2018, Quebec, Quebec, May 2018.

- 8 Detector and Sky Backgrounds, Space Telescope Science Institute, Section 7.4.2 Earthshine, accessible from <http://www.stsci.edu/hst/cos/documents/handbooks/current/ch07.ETC5.html>, accessed 20 May 2018.
- 9 Socrates, <http://www.celestrak.com/SOCRATES/>, accessed Jun 25 2018.
- 10 Space-track.org, <https://www.space-track.org/auth/login>, accessed March 2018.